Journal of Materials Science: Materials in Electronics (2019) 30:11552–11562
https://doi.org/10.1007/s10854-019-01512-9

Effect of flux doped with Cu_6Sn_5 nanoparticles on the interfacial reaction of lead-free solder joints

Haozhong Wang[1] · Xiaowu Hu[1] · Qinglin Li[2] · Min Qu[3]

Received: 9 March 2019 / Accepted: 14 May 2019 / Published online: 18 May 2019

Abstract

In this paper, flux doped with 0.05, 0.1, and 0.2 wt% Cu_6Sn_5 nanoparticles (NPs) were reasonably believed to affect the morphology and growth rate of the intermetallic compounds (IMC) between Cu substrate and Sn–3.0Ag–0.5Cu solder. Reflowing was performed at 250 °C, then isothermal aging was conducted at 150 °C up to 360 h. The experimental results show that the thickness of the IMC layer increased with the increment of aging time. When the aging time extended to 120 h or more, the Cu_3Sn layer appeared on the side of the Cu substrate and also thickened as time increased. The additions of Cu_6Sn_5 NPs into the flux did not change the type of IMCs while the total thickness of the IMC changed visually. It was calculated that the corresponding growth rate constant of interfacial IMCs in solder joints with flux contained 0, 0.05, 0.1, and 0.2 wt% Cu_6Sn_5 NPs were 0.14766, 0.14719, 0.14578 and 0.14726 μm/h$^{1/2}$, respectively. It means that adding Cu_6Sn_5 NPs into flux could effectively inhibit the growth of IMC layer. The strongest inhibition effect on the growth of IMC layer could be achieved when the content of Cu_6Sn_5 NPs was 0.1%. Flux with Cu_6Sn_5 NPs could also effectively inhibit the coarsening of the interfacial IMC grains, and adding 0.1% NPs to the flux has the best inhibition effect.

1 Introduction

The development of modern electronic industry is inseparable from the Pb and its compounds due to its outstanding performance and cheap price. But Pb-based solders are believed to gradually harm our living environment and human health in the last few years because of its toxicity [1–3]. Many efforts have been put into the work to replace the Pb-based solders and numerous lead-free solders have been developed. Nowadays, lead-free solders such as Sn–Ag–Cu, Sn–Bi, Sn–Ag are widely used on account of their non-toxicity and excellent performances. SAC305 (Sn–3.0Ag–0.5Cu) is considered to be the most likely substitute for conventional Sn–Pb solders due to its relatively low melting point, thermal fatigue properties and better compatibility with equipment component [4, 5].

✉ Xiaowu Hu
huxiaowu@ncu.edu.cn

1 School of Mechanical & Electrical Engineering, Nanchang University, Nanchang 330031, China

2 State Key Laboratory of Advanced Processing and Recycling of Nonferrous Metals, Lanzhou University of Technology, Lanzhou 730050, China

3 School of Mechanical and Materials Engineering, North China University of Technology, Beijing 100144, China

However, the long term reliability yet still is concerned to all the researchers. One way to improve the reliability of tin-based solders is to add suitable alloying elements [6–11]. Another way is to add tiny particles to the solder systems [12–14].

The intermetallic compound (IMC) is an important ingredient which forms between solder and metal substrate that can determine the long range reliability of microelectronic packaging. The excessive thickness of IMC will reduce the mechanical properties of solder joints [7, 15]. Morphology of IMC also plays an important role in affecting solder joints. Therefore, the enhancement of solder joint can be achieved through controlling the thickness and the morphology of the interfacial IMC layer.

Among the previous studies and literatures, the addition of nanoparticles were utilized to be an effective method to promote the reliability of solder joint [16–20]. Nanoparticles (NPs) have significant scientific research value because they have advantages in many aspects that other materials do not have. For example, nanomaterials have new properties in terms of optical, magnetic and electrothermal properties [21]; NPs generally have a large specific surface area and relatively high surface tension [22, 23]; The mechanical properties of nanomaterials tend to be superior to other materials [23]. G.K. Sujan and A.S.M.A. Haseeb found that the metallic NPs doped flux successfully had an impact on the solder/substrate interface [15, 24]. They conducted an experiment, in which metal NPs like Ni, Co, Mo and Ti were added to flux. They found that the addition of Ni NPs would increase the wettability of the Sn-based solder, while the additions of Co, Mo, Ti NPs reduced the wettability. On the one hand, the additions of Mo and Ti NPs had little effect on the interfacial IMC morphology, on the other hand, the additions of 0.1 wt% Ni and Co NPs made the interfacial IMC morphology change from scallop-type to flat-type.

Compared with the Sn–Pb solders used in the past, lead-free solders have much lower wettability. The wettability of the solder on the substrate is closely related to the quality of the solder joints and the reliability of the electronic product, so it is important to improve the wettability of the solder [25, 26]. Shen et al. managed to add Ag nanoparticle into the flux [27], they found that the wettability of Sn–3.0Ag–0.5Cu solder on Cu layer was improved on account of the flux doped with Ag NPs, which wetted the solder and covered the surface of the molten solder as a surfactant to promote the effectiveness of the flux during reflowing.

Non-metal NPs like oxide particles can refine the microstructure of solder joints through their addition [28]. Zhang et al. [29] reported that La_2O_3 NPs could reduce the growth rate constant and activation energy of the IMC layer, and the solder joint reliability could be improved after the addition of NPs. The study of Tsao et al. [30] showed that the microstructure of composite solder was improved and the tensile strength of solder was reinforced due to the addition of TiO_2 NPs. After the addition of Fe_2O_3 NPs, the wettability of the solder was improved, and the formation and growth of the IMC layer were suppressed [31].

According to the study of Zhong et al. [32], Cu_6Sn_5 NPs should be a promising low temperature sintering material. Nevertheless, the research on the addition of Cu_6Sn_5 NPs is still relatively rare. In this study, Cu_6Sn_5 NPs were doped into the water soluble flux to investigate its effect on the IMC layer between Cu substrate and SAC305 solder.

2 Experimental procedures

In this study, Cu_6Sn_5 NPs were synthesized through chemical method. The powders of $SnCl_4{\cdot}5H_2O$ and $CuCl_2$ were used as oxidizers, the powder of $NaBH_4$ was used as reductant, the powder of sodium citrate was used as dispersant. The molar ratio of Sn^{4+} and Cu^{2+} should be 6:5 to make sure the formation of Cu_6Sn_5 NPs. After the calculation, 0.86 g of $SnCl_4{\cdot}5H_2O$ and 0.4 g of $CuCl_2$ were completely dissolved in 50 ml deionized water, meanwhile 0.7 g $NaBH_4$ was added into another beaker containing 150 ml deionized water, then 1.5 g sodium citrate was dissolved in the $NaBH_4$ solution to effectively keep the dispersive co-precipitation. After that, the $SnCl_4{\cdot}5H_2O$–$CuCl_2$ solution was dropped into the $NaBH_4$-sodium citrate solution with a constant low speed. To ensure the reaction to

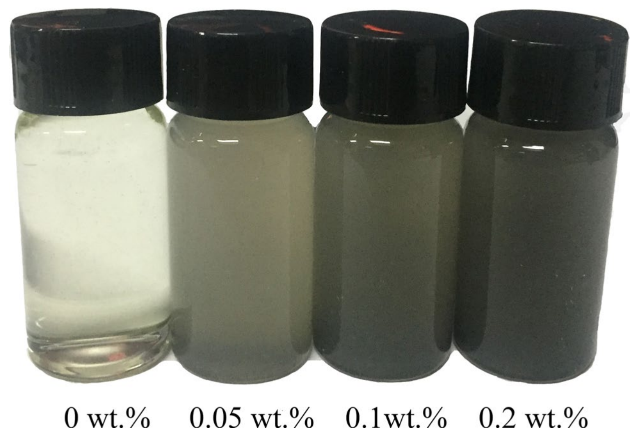

Fig. 2 The fluxes doped with various contents of Cu_6Sn_5 NPs

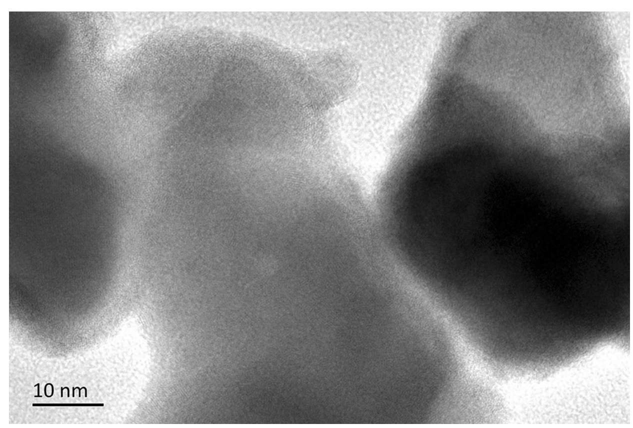

Fig. 3 TEM images of Cu_6Sn_5 NPs

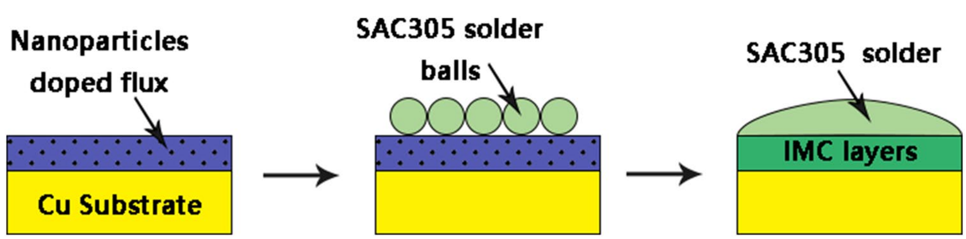

Fig. 1 Schematic diagram of the solder joints using flux doped with Cu_6Sn_5 NPs

be completed, the mixed solution was stirred for 10 min. A centrifuge was used to separate the product with a rotation speed of 2500 r/min, then the remain solution were washed with deionized water and ethanol for three times, respectively. Finally, the product was dried in a vacuum drying oven until the powder of Cu_6Sn_5 NPs were completely dry. The NPs were prepared by the same method mentioned in the study of Hu et al. [33]. Cu_6Sn_5 NPs were characterized through transmission election microscope (TEM).

Figure 1 schematically shows the solder joint using flux doped with NPs. Flux was doped with 0.05, 0.1 and 0.2 wt% Cu_6Sn_5 NPs powders, as shown in the Fig. 2. The composite flux was placed on the surface of Cu sheets ($10 \times 10 \times 2$ mm^3, 99.99% purity) which were ground with sandpaper and polished by a polishing machine. Then lead-free Sn–3.0Ag–0.5Cu solder balls with a diameter of 0.4 mm were placed on the top of Cu sheet. Samples were reflowed in a reflow oven at a constant temperature of 250 °C for 5 min. And then samples were placed in an oven for isothermal aging at 150 °C for 0, 24, 120, 260 and 360 h, respectively. Samples were cut in half, divided into two groups, group 1 and group 2. Scanning Electronic Microscopy (SEM) and

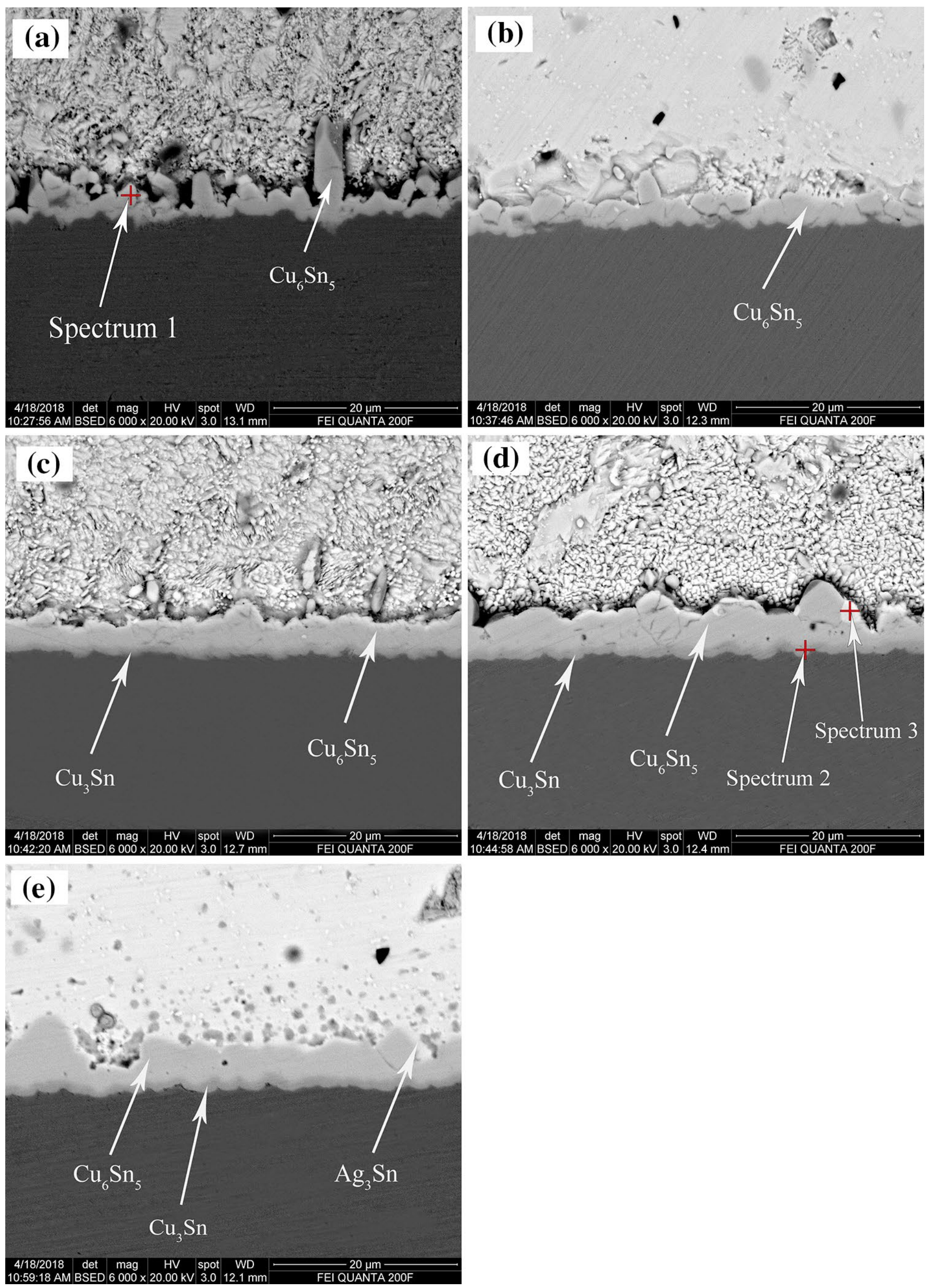

Fig. 4 The SEM images of the cross section structures of SAC305/Cu joints reflowed with undoped flux then aged for **a** 0 h, **b** 24 h, **c** 120 h, **d** 260 h and **e** 360 h

Energy dispersive X-ray spectroscopy (EDS) were used for the observation on the cross section structure of IMC layer between SAC305 solder and Cu substrate of group 1. For purpose of observing the top view of the IMC grains, the surface of samples of group 2 were ground with sandpaper then etched by 20% HNO_3 solution to remove the residual solders.

3 Result and discussion

Figure 3 shows the TEM image of Cu_6Sn_5 NPs, as can be seen from the Fig. 3, the shape of the Cu_6Sn_5 NPs is near-spherical. In addition, the diameters of the Cu_6Sn_5 NPs are measured to be about 30–40 nm. Figure 4a–e show the SEM images of the cross section structures of SAC305/Cu joints treated with undoped flux then aged at 150 °C for (a) 0 h, (b) 24 h, (c) 120 h, (d) 260 h and (e) 360 h, respectively. During reflowing, the interfacial reaction between SAC305 solders and Cu substrate eventually resulted in the formation of Cu_6Sn_5 IMC layer [34]. EDS was used to determine the chemical composition of the IMC layer. Figure 5a shows the composition of the spectrum 1, the weight percentages were 53.73 wt% Cu and 46.27 wt% Sn, respectively, which could be identified as Cu_6Sn_5. A new IMC layer formed between Cu_6Sn_5 IMC layer and Cu substrate when isothermal aging time extended to 120 h. Figure 5b shows the composition of the spectrum 2 (composited of 76.11 wt% Cu and 23.89 wt% Sn) which was identified as Cu_3Sn, so that Cu_6Sn_5 and Cu_3Sn IMC layers appeared at the interface of SAC305/Cu joint as the aging time extended to 120 h. The Cu_3Sn IMC layer was produced by following reactions of $Cu + Sn \rightarrow Cu_3Sn$ and $Cu + Cu_6Sn_5 \rightarrow Cu_3Sn$ [33], because the growth of Cu_3Sn was

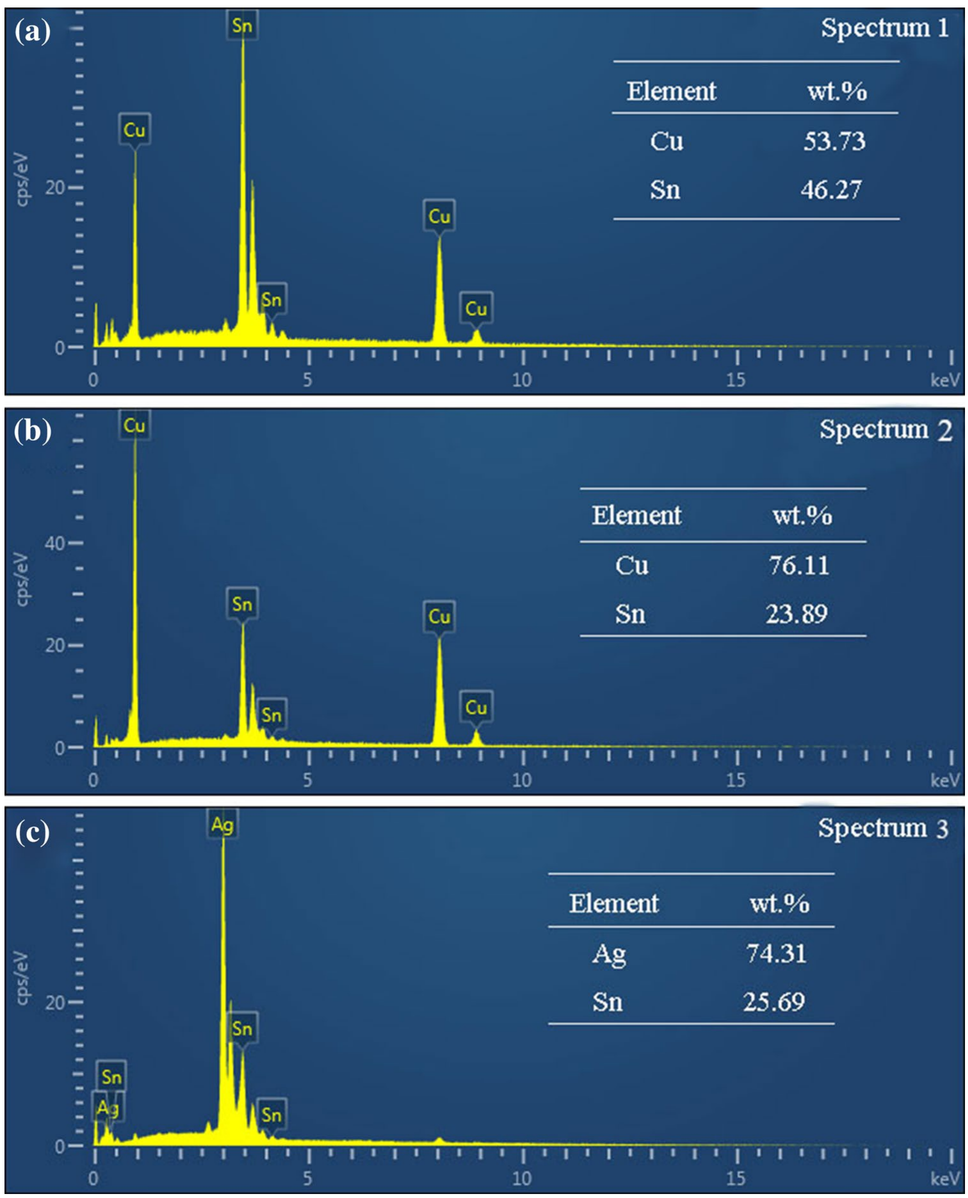

Fig. 5 Cross-section EDS analysis of SAC305/Cu joints treated with undoped flux, **a** spectrum 1, **b** spectrum 2 and **c** spectrum 3

considered as a diffusional and a reactive type [35], therefore the formation of Cu_3Sn required more reaction time. It is clearly seen from Fig. 4a that the morphology of Cu_6Sn_5 IMC layer is scallop-type when aging time was relatively short. The IMC layers transformed form scallop type to planer type when the aging time increased, as shown in Fig. 4a–e. It can also be seen that a white spot-like phase appeared on the interface between the IMC layer and the solder as the aging time extended to 24 h, Fig. 5c exhibits the composition of the spectrum 3 (composited of 74.31 wt% Ag and 25.69 wt% Sn), which indicated that the ingredient of the spectrum 3 was Ag_3Sn, this phenomenon has already been mentioned in the previous literature. Ag_3Sn was produced by the combination of Ag and Sn atoms diffusing from the solder. Furthermore, the thickness of Cu_3Sn layer and Cu_6Sn_5 layer gradually increased with the prolongation of aging time and the thickness of total IMC layers was determined to be (a) 2.96 μm, (b) 3.12 μm, (c) 4.04 μm, (d) 5.25 μm and (e) 5.53 μm.

The SEM images of the cross section structures of SAC305/Cu joints treated with flux containing 0.05 wt% Cu_6Sn_5 NPs and then aged at 150 °C for (a) 0 h, (b) 24 h, (c) 120 h, (d) 260 h and (e) 360 h are shown in Fig. 6a–e. The Cu_6Sn_5 IMC

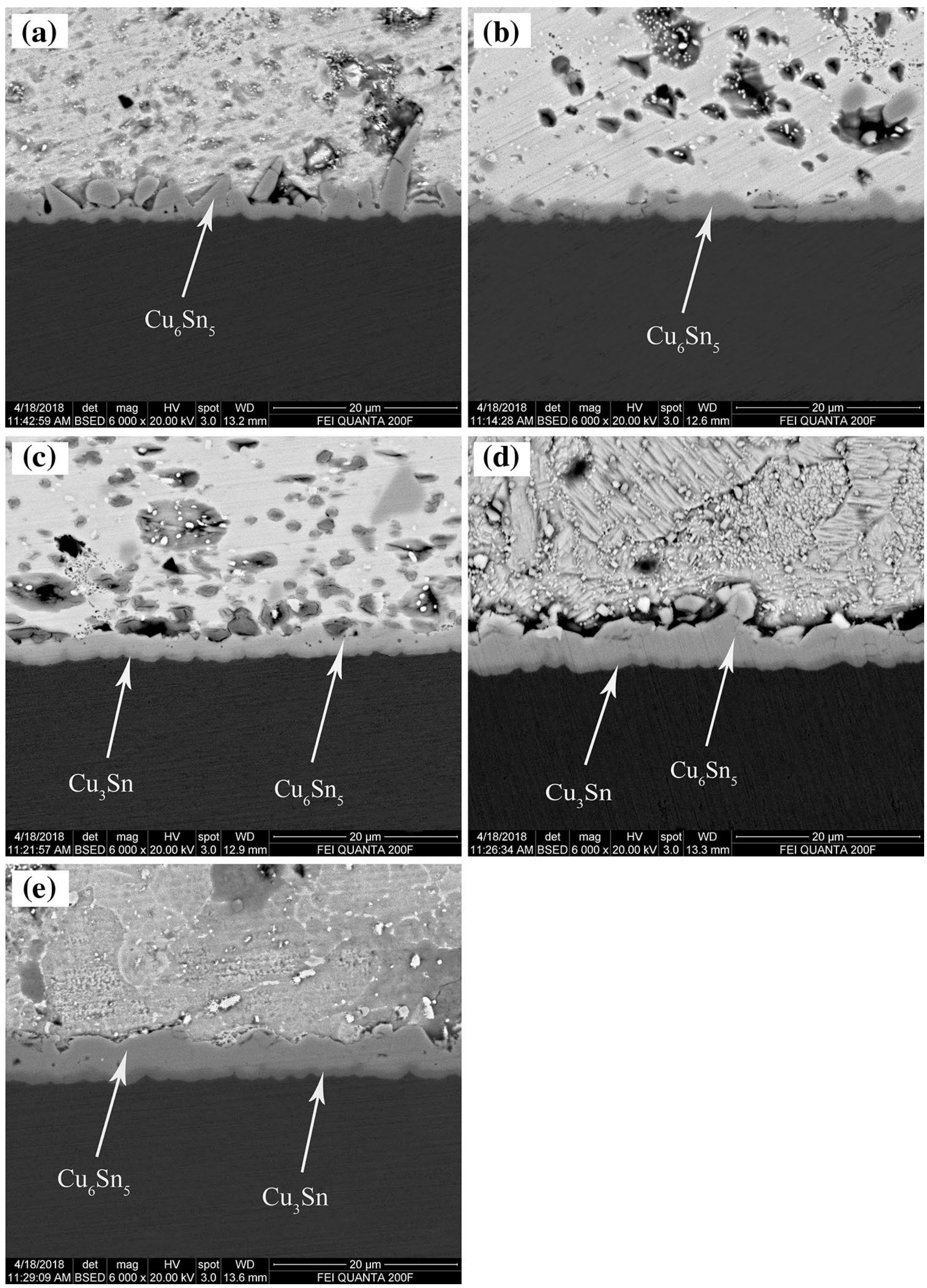

Fig. 6 The SEM images of the cross section structures of SAC305/Cu joints reflowed with flux containing 0.05 wt% Cu_6Sn_5 NPs **a** 0 h, **b** 24 h, **c** 120 h, **d** 260 h and **e** 360 h

layer appeared during reflow process, the appearance of Cu_3Sn IMC layer after 120 h of aging proves that the appearance time of Cu_3Sn layer does not change with the addition of Cu_6Sn_5 NPs. The morphology of the IMC layer converted from scallop-type to planer-type with aging time extended from 0 to 360 h, therefore, the additions of NPs did not alter the morphology of the IMC layer. The thickness of Cu_6Sn_5 IMC layer and Cu_3Sn IMC layer both increased with the extension of aging time. The total thickness of IMC layer increased significantly and the thicknesses were measured as (a) 1.58 μm,(b) 2.80 μm, (c) 3.25 μm, (d) 3.70 μm and (e) 3.85 μm.

Figures 7a–e and 8a–e show the morphologies of the IMC layer of SAC305/Cu joints treated with flux containing 0.1 wt% and 0.2 wt% Cu_6Sn_5 NPs. The emergence, morphology and growth of Cu_6Sn_5 IMC layer and Cu_3Sn IMC layer were accordant with previous rule, Cu_6Sn_5 IMC layer was produced between solder and Cu substrate during reflowing. Cu_3Sn IMC layer was appeared when the aging time has reached 120 h. The IMC layer morphology changed from scallop-like to planer-like. The thickness of Cu_6Sn_5 and Cu_3Sn IMC layers increased gradually. The thickness of IMC layer of the solder joints treated with flux containing

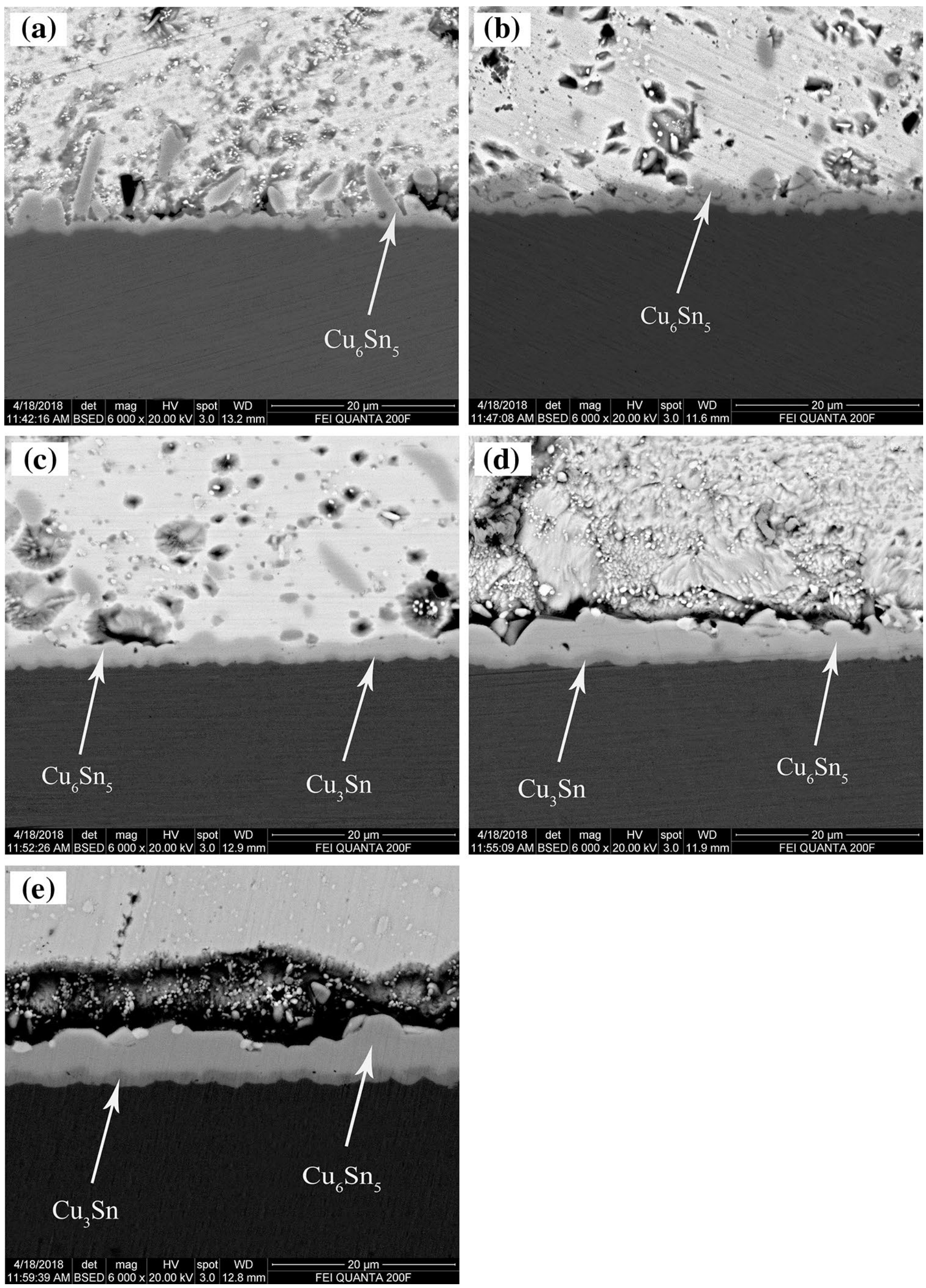

Fig. 7 The SEM images of the cross section structure of SAC305/Cu joints reflowed with flux containing 0.1 wt% Cu_6Sn_5 NPs **a** 0 h, **b** 24 h, **c** 120 h, **d** 260 h and **e** 360 h

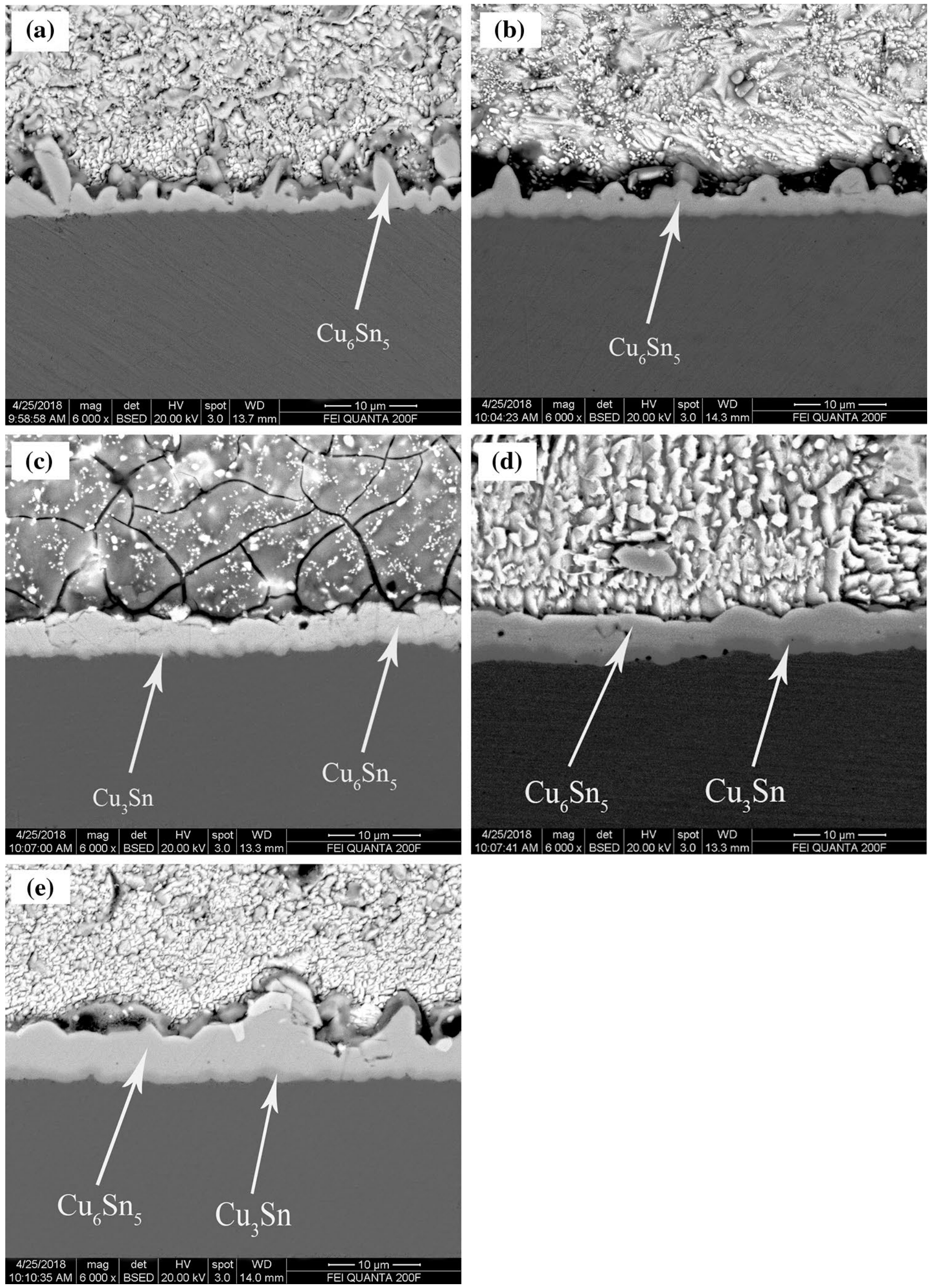

Fig. 8 The SEM images of the cross section structures of SAC305/Cu joints reflowed with flux containing 0.2 wt% Cu_6Sn_5 NPs **a** 0 h, **b** 24 h, **c** 120 h, **d** 260 h and **e** 360 h

0.1 wt% and 0.2 wt% Cu_6Sn_5 NPs were determined to be 1.77, 1.88, 2.85, 3.76, and 4.46 μm (0.1 wt%) and 2.60, 2.89, 3.91, 4.52 and 5.30 μm (0.2 wt%), respectively.

Table 1 presents the average thickness of IMC layers in solder joints treated with flux containing multiple groups of Cu_6Sn_5 NPs after different aging time. The growth kinetics of IMC layer during isothermal aging is controlled by diffusion mechanism, which can be described as a formula [36, 37]:

$$X = X_0 + At^n \tag{1}$$

Table 1 Average thickness of IMC layers in solder joints treated with flux containing various contents of Cu_6Sn_5 NPs under different aging time

Nanoparticle mass fraction (%)	The average thickness of IMC layer (μm)				
	0 h	24 h	120 h	260 h	360 h
0	2.96	3.12	4.04	5.25	5.53
0.05	2.20	2.32	3.08	4.49	4.75
0.1	1.77	1.88	2.85	3.76	4.46
0.2	2.60	2.89	3.91	4.52	5.30

where X represents the total thickness of IMC layer at the aging time t, X_0 represents the thickness of IMC layer after reflow process. A represents the growth rate constant and n represents time index. Previous studies have shown that the growth of the IMC layer follows parabolic dynamics, which indicates that the growth is controlled by volume diffusion mechanism. Thus, the time index n can be 0.5.

Figure 9 demonstrates the linear relationship between the total thickness of interfacial IMC layers in four different kinds of solder joints and the square root of isothermal aging time. The growth rate constant of interfaical IMC of samples treated with flux containing different mass fraction of Cu_6Sn_5 NPs (0 wt%, 0.05 wt%, 0.1 wt% and 0.2 wt%) were determined to be 0.14766, 0.14719, 0.14578 and 0.14726 μm/h$^{1/2}$. When the content of Cu_6Sn_5 NPs increased from 0 to 0.1 wt%, the growth rate constant increased, and when the content of Cu_6Sn_5 NPs increased from 0.1 to 0.2 wt%, the growth rate constant reduced, but compared with the Cu_6Sn_5 NPs-free flux, the growth rate constant of the solder joints treated with flux containing 0.2 wt% Cu_6Sn_5 NPs was smaller. The result indicates that the addition of Cu_6Sn_5 NPs into flux could inhibit the growth of IMC layer, and the most obvious inhibition effect could be achieved when the content of Cu_6Sn_5 NPs was 0.1 wt%.

Similar phenomenon was mentioned in previous study [38], in the case of SAC305-xTiO_2 (x = 0, 0.02, 0.05, 0.1, 0.3 and 0.6 wt%) solder joints reflowed for 3600 s, the thickness of IMC layer decreased with the increment of the mass fraction of TiO_2 NPs. This situation continued until the mass fraction of TiO_2 NPs reached 0.1 wt%. A further increment in the concentration of TiO_2 NPs would result in the thickening of the IMC layer, which revealed that the inhibition effect on the IMC layer was most effective when the content of TiO_2 NPs was about 0.1 wt%. According to the work of Gu et al. [31], the inhibition effect on the IMC layers is attributed to the ability of the interface between solder/substrate to adsorb NPs. With the increment of the amount of NPs, the adsorption ability also increased, therefore the suppression effect was getting better. The NPs would gather together and turn into larger particles when the mass fraction of NPs surpassed the criticality value. As a result, the adsorption ability of interface on NPs was reduced.

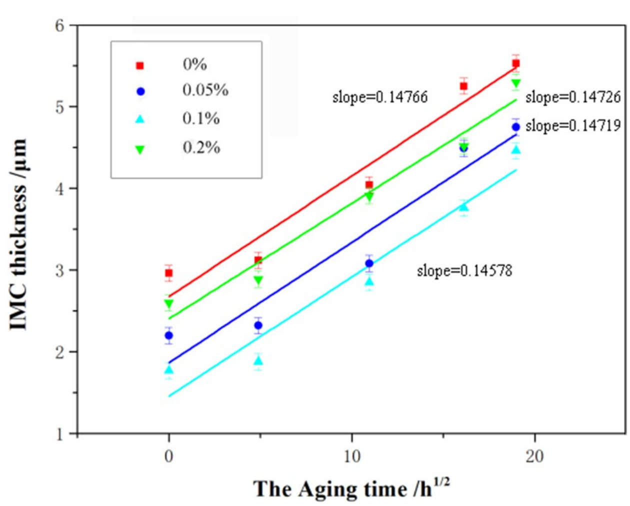

Fig. 9 The linear relationship between the total thickness of IMC layers in four groups of solder joints and the square root of isothermal aging time

Figure 10a–d show the IMC grains of solder joints treated with flux containing (a) 0 wt%, (b) 0.05 wt%, (c) 0.1 wt% and (d) 0.2 wt% Cu_6Sn_5 NPs and then aged at 150 °C for 24 h and Fig. 10e–h show the IMC grains of solder joints treated with flux containing (e) 0 wt%, (f) 0.05 wt%, (g) 0.1 wt% and (h) 0.2 wt% Cu_6Sn_5 NPs and then aged for 260 h. It is seen from Fig. 10a–h that the diameters of IMC grains increased as the aging time increased. The work of Yang et al. [39] reported that the relationship between the diameter of IMC grains and aging time can be describe as following formula:

$$d = Ct^{1/3} \tag{2}$$

where d represents the diameter of IMC grains, C represents the growth coefficient of IMC grains and t represents the aging time. According to the Table 2, Fig. 11 illustrates the liner relationship between the diameter of IMC grains and cube root of aging time. The growth coefficient of IMC grains of samples treated with flux containing different mass fraction of Cu_6Sn_5 NPs (0, 0.05, 0.1 and 0.2 wt%) were determined to be 0.38376, 0.31401, 0.28515 and 0.3724 μm/h$^{1/3}$. The flux contained Cu_6Sn_5 NPs had the same inhibition effect on the growth of IMC grain as on the growth of IMC layer. Whether the growth of IMC grains or the growth of the IMC layer, the restraining effect was most significant when 0.1 wt% Cu_6Sn_5 NPs were added into the flux.

Liu et al. [40] found that the addition of 0.01 wt% and 0.05 wt% SiC NPs into the composite solder could inhibit the growth of IMC grains, however, the IMC grains had the same size when the solder was added with 0.2 wt% and 0.01 wt% SiC NPs. This may be due to the van der Waals forces made the SiC NPs entangle with each other when the weight percentage of SiC NPs achieved 0.2 wt%, reducing the inhibition effect of IMC grains diameter. In summary, the increment of the weight percentage of Cu_6Sn_5 NPs could increase the adsorption of NPs by the interface, which could inhibit the growth of IMC grains. But when the concentration of Cu_6Sn_5 NPs reached a certain level, the NPs become entangled with each other and reduced the adsorption ability of NPs by the interface, therefore the suppression effect on the IMC grains were weakened.

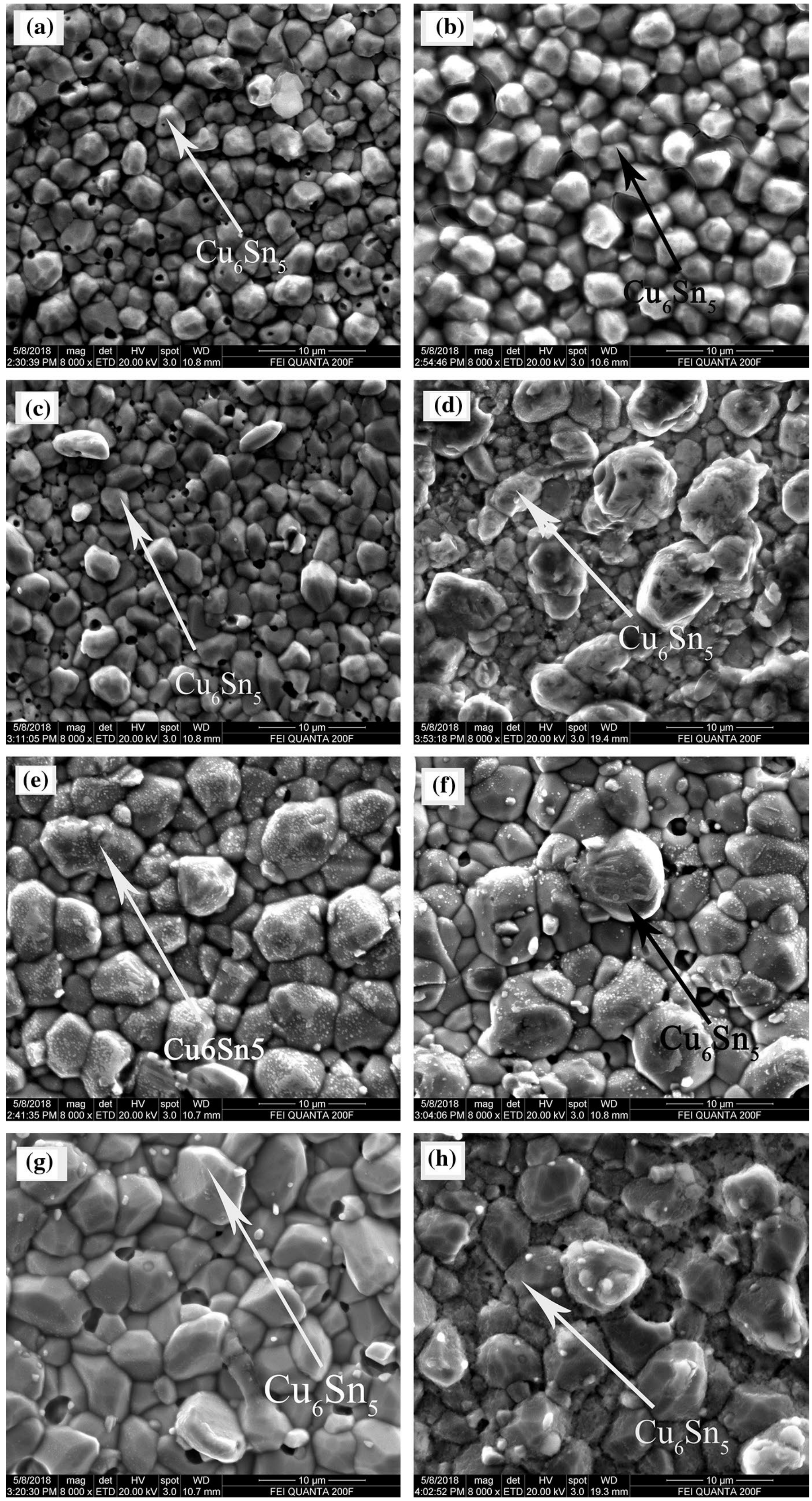

Fig. 10 The IMC grains of solder joints reflowed with flux containing **a** 0 wt%, **b** 0.05 wt%, **c** 0.1 wt%, **d** 0.2 wt%, **e** 0 wt%, **f** 0.05 wt%, **g** 0.1 wt% and **h** 0.2 wt% Cu_6Sn_5 NPs then aged for **a**–**d** 24 h; **e**–**h** 260 h

Table 2 The diameter of IMC grains of samples processed with flux containing various contents of Cu_6Sn_5 NPs under different aging time

Nanoparticle mass fraction (%)	The diameter of IMC grains (μm)				
	0 h	24 h	120 h	260 h	360 h
0	1.73	3.00	3.40	4.30	4.50
0.05	1.58	2.80	3.25	3.70	3.85
0.1	1.55	2.51	3.08	3.39	3.60
0.2	1.60	2.88	3.31	4.11	4.41

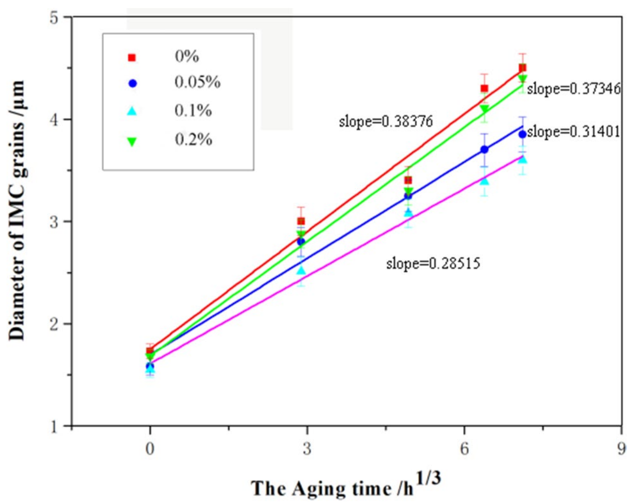

Fig. 11 The liner relationship between the diameter of IMC grains and cube root of aging time

4 Conclusions

(1) The Cu_6Sn_5 IMC layer appeared on the interface between solder and Cu substrate during reflowing, Cu_3Sn IMC layer appeared between Cu_6Sn_5 IMC layer and Cu substrate when aging time extended to around 120 h. The IMC layers were transformed from scallop type to planer type, besides, the thickness of Cu_3Sn IMC layer and Cu_6Sn_5 IMC layer increased with the prolongation of aging time.

(2) The inhibition effect on the thickness of IMC layer of solder joints reflowed with flux containing Cu_6Sn_5 NPs during reflow process was significant. What's more, the flux doped with 0.1 wt% Cu_6Sn_5 NPs had the most obvious inhibitory effect on the growth of IMC layer. The growth rate constant of solders were 0.14766, 0.14719, 0.14578 and 0.14726 μm/h$^{1/2}$, respectively.

(3) The coarsening of IMC grains was restrained after Cu_6Sn_5 NPs were added into flux. The inhibition effect on the growth of IMC grains was most conspicuous when flux was doped with 0.1 wt% Cu_6Sn_5 NPs.

Acknowledgements This work was supported by the Nature Science Foundation of China (Grant No. 51765040), Nature Science Foundation of Jiangxi Province (Grant No. 20161BAB206122).

References

1. H.Y. Jing, H.J. Guo, L.X. Wang, J. Wei, L.Y. Xu, Y.D. Han, Influence of Ag-modified graphene nanosheets addition into Sn-Ag-Cu solders on the formation and growth of intermetallic compound layers. J. Alloys Compd. **702**, 669–678 (2017)
2. L.Y. Xu, X. Chen, L.X. Wang, H.Y. Jing, J. Wei, Y.D. Han, Design and performance of Ag nanoparticle-modified graphene/SnAgCu lead-free solders. Mater. Sci. Eng., A **667**, 87–96 (2016)
3. F.J. Wang, H. Chen, Y. Huang et al., Recent progress on the development of Sn-Bi based low-temperature Pb-free solders. J. Mater. Sci. Mater. Electron. **30**, 3222–3243 (2019)
4. W.M. Chen, S.K. Kang, C.R. Kao, Effects of Ti addition to Sn-Ag and Sn-Cu solders. J. Alloys Compd. **520**, 244–249 (2012)
5. Y. Zhang, H. Zhu, M. Fujiwara, J. Xu, M. Dao, Low-temperature creep of SnPb and SnAgCu solder alloys and reliability prediction in electronic packaging modules. Sci. Mater. **68**, 607–610 (2013)
6. Y.W. Wang, T.L. Yang, J.Y. Wu, C.R. Kao, Pronounced effects of Zn additions on Cu-Sn microjoints for chip-stacking applications. J. Alloys Compd. **750**, 570–576 (2018)
7. F. Sun, P. Hochstenbach, W.D.V. Driel, G.Q. Zhang, Fracture morphology and mechanism of IMC in low-Ag SAC solder/UBM(Ni(P)–Au) for WLCSP. Microelectron. Reliab. **48**, 1167–1170 (2008)
8. C. Yang, Y. Song, S.W.R. Lee, Impact of Ni concentration on the intermetallic compound formation and brittle fracture strength of Sn–Cu–Ni (SCN) lead-free solder joints. Microelectron. Reliab. **54**, 435–446 (2014)
9. I.E. Anderson, J.L. Harringa, Suppression of void coalescence in thermal aging of tin-silver-copper-X solder joints. J. Electron. Mater. **35**, 94–106 (2006)
10. J. Hu, A. Hu, M. Li, D. Mao, Depressing effect of 0.1 wt% Cr addition into Sn-9Zn solder alloy on the intermetallic growth with Cu substrate during isothermal aging. Mater. Charact. **61**, 355–361 (2010)
11. Y.W. Wang, C.C. Chang, C.R. Kao, Minimum effective Ni addition to SnAgCu solders for retarding Cu_3Sn growth. J. Alloys Compd. **478**, L1–L4 (2009)
12. Y. Tang, G.Y. Li, T.C. Pan, Influence of TiO_2 nanoparticles on IMC growth in Sn-3.0Ag-0.5Cu–xTiO_2 solder joints in reflow process. J. Alloys Compd. **554**, 195–203 (2013)
13. A.S.M.A. Haseeb, M.M. Arafat, M.R. Johan, Stability of Molybdenum nanoparticles in Sn-3.8Ag-0.7Cu solder during multiple reflow and their influence on interfacial intermetallic compounds. Mater. Charact. **64**, 27–35 (2012)
14. C.A. Yang, S. Yang, X. Liu, C.R. Kao, Enhancement of nano-silver chip attachment by using transient liquid phase reaction with indium. J. Alloys Compd. **762**, 586–597 (2018)
15. G.K. Sujan, A.S.M.A. Haseeb, A.B.M. Afifi, Effects of metallic nanoparticle doped flux on the interfacial intermetallic compounds between lead-free solder ball and copper substrate. Mater. Charact. **97**, 199–209 (2014)
16. Z. Fathian, A. Maleki, B. Niroumand, Synthesis and characterization of ceramic nanoparticles reinforced lead-free solder. Ceram. Int. **43**, 5302–5310 (2017)
17. Y. Wen, X. Zhao, Z. Chen et al., Reliability enhancement of Sn-1.0Ag-0.5Cu nano-composite solders by adding multiple sizes of TiO_2, nanoparticles. J. Alloys Compd. **696**, 799–807 (2017)

18. Z. Zhao, L. Liu, H.S. Choi et al., Effect of nano-Al_2O_3 reinforcement on the microstructure and reliability of Sn-3.0Ag-0.5Cu solder joints. Microelectron. Reliab. **60**, 126–134 (2016)
19. B. Philippi, K. Matoy, J. Zechner et al., Fracture toughness of intermetallic Cu_6Sn_5, in lead-free solder microelectronics. Scr. Mater. **123**, 38–41 (2016)
20. L.C. Tsao, S.Y. Chang, C.I. Lee et al., Effects of nano-Al_2O_3 additions on microstructure development and hardness of Sn-3.5Ag-0.5Cu solder. Mater. Des. **31**, 4831–4835 (2010)
21. X.J. Wu, Z.Q. Wei, L.L. Zhang et al., Optical and magnetic properties of Fe Doped ZnO nanoparticles obtained by hydrothermal synthesis. J. Nanomater. **9**, 1–6 (2014)
22. F. Bødker, S. Mørup, S. Linderoth, Surface effects in metallic iron nanoparticles. Phys. Rev. Lett. **72**, 282–285 (1994)
23. K.K. Nanda, A. Maisels, F.E. Kruis, H. Fissan, S. Stappert, Higher surface energy of free nanoparticles. Phys. Rev. Lett. **91**, 106102 (2003)
24. G.K. Sujan, A.S.M.A. Haseeb, H. Nishikawa, M.A. Amalina et al., Interfacial reaction, ball shear strength and fracture surface analysis of lead-free solder joints prepared using cobalt nanoparticle doped flux. J. Alloys Compd. **695**, 981–990 (2017)
25. M. Abtew, G. Selvaduray, Lead-free solders in microelectronics. Mater. Sci. Eng., R **27**, 95–141 (2000)
26. H.Y. Chang, S.W. Chen, D.S.H. Wong, H.F. Hsu, Determination of reactive wetting properties of Sn, Sn-Cu, Sn-Ag, and Sn-Pb alloys using a wetting balance technique. J. Mater. Res. **18**, 1420–1428 (2003)
27. J. Shen, Y.C. Chan, Effect of metal/ceramic nanoparticle-doped fluxes on the wettability between Sn-Ag-Cu solder and a Cu layer. J Alloys Compd. **477**, 909–914 (2009)
28. X. Li, Y. Ma, W. Zhou et al., Effects of nanoscale Cu_6Sn_5, particles addition on microstructure and properties of SnBi solder alloys. Mater. Sci. Eng., A **684**, 328–334 (2017)
29. L. Zhang, L.L. Gao, Interfacial compounds growth of SnAgCu(nano La_2O_3)/Cu solder joints based on experiments and FEM. J Alloys Compd. **635**, 55–60 (2015)
30. L.C. Tsao, C.H. Huang, C.H. Chung, R.S. Chen, Influence of TiO_2 nanoparticles addition on the microstructural and mechanical properties of Sn0.7Cu nano-composite solder. Mater. Sci. Eng. A **545**, 194–200 (2012)
31. Y. Gu, X. Zhao, Y. Li et al., Effect of nano-Fe_2O_3, additions on wettability and interfacial intermetallic growth of low-Ag content Sn-Ag-Cu solders on Cu substrate. J. Alloy. Compd. **627**, 39–47 (2015)
32. Y. Zhong, R. An, C. Wang, Z. Zheng et al., Low temperature sintering Cu_6Sn_5 nanoparticles for superplastic and super-uniform high temperature circuit interconnections. Small **11**, 4097–4103 (2015)
33. X.X. Hu, Y. Qiu, X.X. Jiang et al., Effect of Cu_6Sn_5, nanoparticle on thermal behavior, mechanical properties and interfacial reaction of Sn-3.0Ag-0.5Cu solder alloys. J. Mater. Sci.: Mater. Electron. **29**, 15983–15993 (2018)
34. C.T. Heycock, F.H. Neville, On the constitution of copper-tin alloys. Proc. R. Soc. London. **69**, 320–329 (1901)
35. T. Laurila, V. Vuorinen, J.K. Kivilahti, Interfacial reactions between lead-free solders and common base materials. Cheminform. **49**, 1–60 (2005)
36. J. Shen, M.L. Zhao, P.P. He et al., Growth behaviors of intermetallic compounds at Sn-3.0Ag-0.5Cu/Cu interface during isothermal and non-isothermal aging. J. Alloys Compd. **574**, 451–458 (2013)
37. M. Yang, Y.H. Ko, J. Bang et al., Growth inhibition of interfacial intermetallic compounds by pre-coating oriented Cu_6Sn_5 grains on Cu substrates. J. Alloys Compd. **701**, 533–541 (2017)
38. Y. Tang, G.Y. Li, Y.C. Pan, Influence of TiO_2 nanoparticles on IMC growth in Sn-3.0Ag-0.5Cu-xTiO_2 solder joints in reflow process. J. Alloys Compd. **554**, 195–203 (2013)
39. H.M. Yang, M.Y. Li, J.Y. Kim, Texture evolution and its effects on growth of intermetallic compounds formed at eutectic $Sn_{37}Pb$/Cu interface during solid-state aging. Intermetallics **31**, 177–185 (2012)
40. P. Liu, P. Yao, J. Liu, Effect of SiC nanoparticle additions on microstructure and microhardness of Sn-Ag-Cu solder alloy. J. Electron. Mater. **37**, 874–879 (2008)